Available online at www.sciencedirect.com
ScienceDirect
Journal of Hazardous Materials 146 (2007) 58–64
Journal of Hazardous Materials
www.elsevier.com/locate/jhazmat

Mechanisms and kinetics of chelating reaction between novel chitosan derivatives and Zn(II)

Ping Ding, Ke-Long Huang *, Gui-Yin Li, Wen-Wen Zeng

College of Chemistry and Chemical Engineering, Central South University, Changsha 410083, PR China

Received 28 August 2006; received in revised form 21 November 2006; accepted 24 November 2006
Available online 15 December 2006

Abstract

Modified chitosan such as chitosan alpha-ketoglutaric acid (KCTS) and hydroxamated chitosan alpha-ketoglutaric acid (HKCTS) are successfully prepared. The resulting polymers were characterized by ^{13}C NMR and X-ray diffraction (XRD), respectively. A adsorption system was applied to study the adsorption of Zn(II) ion onto chitosan derivatives. The isothermal sorption kinetics of chitosan derivatives for Zn(II) ion has been investigated. The kinetics experimental data correlated well with the second-order kinetic model, indicating that the chemical sorption was the rate-limiting step. The adsorption mechanism of chitosan derivatives with Zn(II) was studied by Fourier transform infrared spectroscopy (FT-IR) and X-ray photoelectron spectroscopy (XPS). The results indicated that the nitrogen in amino group and the oxygen in carboxyl group of KCTS were coordination atoms. N atom of amino group, O atom of hydroxamic acid and O atom of carbonyl group in HKCTS coordinated with Zn(II).

Keywords: Chitosan derivatives; Chelating reaction; Adsorption isotherm; Zn(II) ion

1. Introduction

Chitosan, a naturally abundant biopolymer, is non-toxic, biodegradable and biocompatible. Different from most other natural polymers, chitosan has high reactivity and process ability for its specific molecular structure and polycationic nature [1,2]. Chitosan has been reported to have high potential for adsorption of metal ions [3,4], dyes [5] and proteins [6]. Chitosan is a powerful chelating agent, which is easy to form complexes with transition metals and heavy metals. Recent years, most researches of chitosan derivatives-metal complexes focused on their applications in the sequestration or removal of metal ions, dyeing, catalysis, water treatment, and many other industrial processes [7]. The problem of heavy metal ions removal with use of chitinous materials is widely reported in the literature [8–10], but the potential the materials offer is so high that it deserves continual research efforts.

This work concentrates on the study of Zn(II) ions sorption onto chitosan derivatives, and the isothermal sorption kinetics of chitosan derivatives for Zn(II) ion has been investigated. The adsorption rates were determined quantitatively and compared by the first-order, second-order and the intraparticle diffusion model. The adsorption mechanism of chitosan derivatives with Zn(II) was studied by infrared spectral analysis and X-ray photoelectron spectroscopy analysis. This information will be useful for further applications of system design in the sequestration or removal of metal ions and many other industrial processes.

2. Experimental

2.1. Chemicals

Chitosan (CTS, MW4.9 × 105, degree of deacetylation: 95%) was procured from Dalian Xindie Chitin Co., Ltd. Theophylline was provided by Qingdao Medicine Institute. alpha-Ketoglutaric acid was purchased from Qianshan Science and Technology Development Company, Zhuhai of China. The other reagents were of analytical grade and used without further purification. All solutions were prepared with deionized water.

2.2. Synthesis of KCTS

CTS (4.5 g) was dissolved in 100 ml of 1 wt% acetic acid, alpha-ketoglutaric acid (7.2 g) was added to CTS. The pH of the

* Corresponding author.
E-mail address: klhuang@mail.csu.edu.cn (K.-L. Huang).

0304-3894/$ – see front matter © 2007 Elsevier B.V. All rights reserved.
doi:10.1016/j.jhazmat.2006.11.061

solution was adjusted to 4.5–5.0 using sodium hydroxide solution. Afterwards, sodium borohydride was added to the stirred mixture at 37 °C. The pH of the polymeric solution was adjusted to 6.5–7.0 using hydrochloric acid solution and the reaction was further stirred for 24 h. The reaction was terminated by 95% alcohol, the precipitated polymer was filtered, washed three to four times with ethanol and diethyl ether, respectively. The product was dried in an infrared drier.

2.3. Synthesis of HKCTS

KCTS (4.5 g) was dissolved in water (100 ml). Subsequently, the pH of the polymeric solution was adjusted to 4.0–4.5 using hydrochloric acid solution (1.0N). Afterwards, dicyclohexylcarbodiimide (DCCI, 0.74 g) was added to the stirred mixture. Two hours later, hydroxylamine hydrochloride (4.5 g) was added and the reaction was further stirred for 1 h. Then the pH of the solution was adjusted and the reaction mixture was stirred over 24 h at room temperature. The precipitated polymer was filtered, washed three to four times with ethanol, followed by acetone and diethyl ether, respectively. The polymer was dried in an infrared drier.

2.4. Characterization

The FT-IR spectra were obtained in KBr disk on a Hitachi 270-50 FT-IR Spectrophotometer. The polymer samples were solubilized in CF_3COOD/D_2O (3%, w/w) and spectra of ^{13}C NMR were obtained in 400 MHz with a Varian 300 M Inova NMR spectroscopy instrument downfield from tetramethylsilane. X-ray diffraction diagrams were recorded with a Japan Rigaku D/Max-2550VB$^+$ 18 kW X-ray diffractometer using graphite-monochromatized Cu Kα radiation ($k = 1.54178$ Å). XPS spectra were taken by VGESCALAB MKII spectrometer equipped with an Al Kα X-ray source.

2.5. Batch adsorption experiments

Batch adsorption experiments were conducted by placing 10 g of the chitosan derivatives in a 150 ml flask with 75 ml zinc sulfate solution of a known initial concentration. The mixture in the flask was shaken at room temperature on an orbit shaker operated at 100 rpm for a period of up to 60 min or until adsorption equilibrium was established. The initial pH of the solutions was adjusted with sodium hydroxide solution to 6.0. The histories of Zn(II) ion concentration in the solutions were determined by taking and analyzing solution samples periodically. The adsorbed amount of Zn(II) ion per unit weight of chitosan derivatives at time t, $q(t)$ (mg g^{-1}) was calculated from the mass balance equation as:

$$q(t) = \frac{(c_0 - c_t)V}{m} \quad (1)$$

where c_0 and c_t (mg l^{-1}) are the initial Zn(II) ion concentration and the Zn(II) ion concentrations at any time t, respectively; V the volume of the Zn(II) ion solution; and m is the weight of the chitosan derivatives.

3. Results and discussion

Fig. 1 shows a schematic representation of the preparation of KCTS and HKCTS.

3.1. X-ray diffraction (XRD) analysis of CTS, KCTS and HKCTS

Fig. 2 shows the X-ray diffraction (WAXD) patterns of CTS, KCTS, and HKCTS. The wide-angle X-ray diffraction pattern of CTS showed the characteristic peaks at $2\theta = 10°, 20°$. For KCTS the characteristic peak at $2\theta = 10°, 20°$ decreased. For HKCTS the intensity of the characteristic peak at $2\theta = 10°, 20°$ decreased more than that of KCTS. It was thought that the decrease in crystallinity of KCTS could be attributed to the deformation of the strong hydrogen bond in the chitosan backbone chain, as the amino groups were substituted by alpha-ketoglutaric acid. In addition, the decrease in crystallinity of HKCTS because of the carboxyl groups in the KCTS reacted with hydroxylamine hydrochloride also. Both KCTS and HKCTS had low crystallinity, indicating that they were considerably more amorphous than was CTS. Numerous open pores have been observed on the surface of chitosan derivatives with sizes ranging from about 0.1 to 1.0 μm under a scanning electron microscope (model KYKY2800, China). Pore size was improved and the adsorption capacity can be enhanced by these modifications. The mean par-

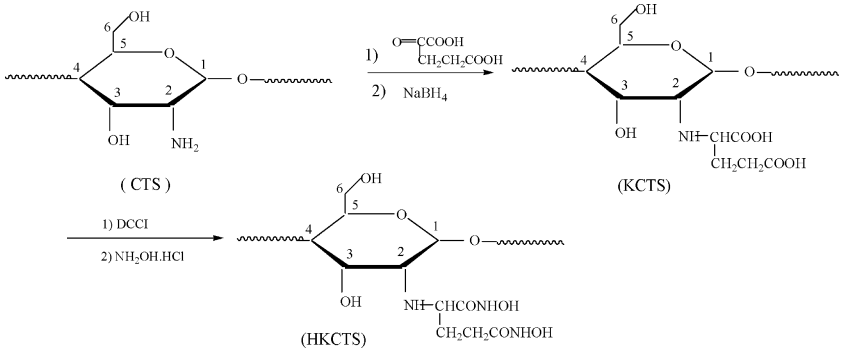

Fig. 1. Synthetic route of KCTS and HKCTS.

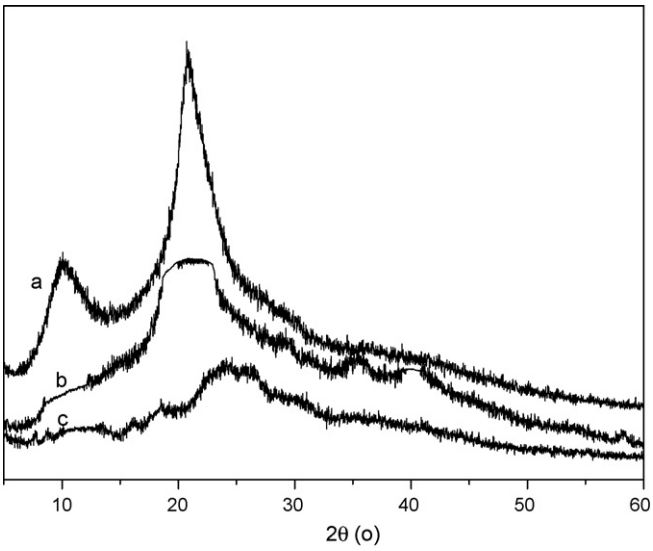

Fig. 2. X-ray diffraction patterns of CTS (a), KCTS (b) and HKCTS (c).

ticle sizes were measured to be 100 μm for KCTS, 110 μm for HKCTS, respectively, using a laser-based particle size analyzer (Galai, CIS-1, Israe).

3.2. Nuclear magnetic resonance analysis of CTS, KCTS and HKCTS

More information about the chitosan derivatives was obtained by ^{13}C NMR analysis. The ^{13}C NMR spectrum of CTS, KCTS and HKCTS were shown in Fig. 3.

The spectrum of CTS is the same as that reported by Zong et al. [11]. In comparison with CTS, ^{13}C NMR spectrum of KCTS, three signals at 168.2, 53.8 and 39.7 ppm were attributed to carbonyl carbons, methyne carbons and methylene carbons, respectively. This indicates chitosan is successfully modified by alpha-ketoglutaric acid. ^{13}C NMR spectrum of HKCTS, three signals at 169.6, 54.1 and 40.6 ppm were attributed to hydroxamic carbonyl carbons, methyne carbons and methylene carbons, respectively. Considering this NMR analysis, it is possible now to identify the chitosan derivatives obtained and to relate their structure to the preparation conditions.

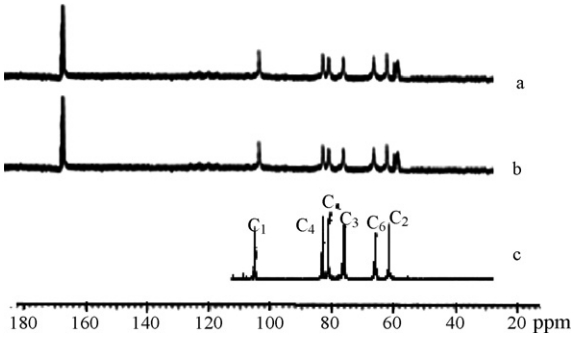

Fig. 3. ^{13}C NMR spectra of CTS (a), KCTS (b) and HKCTS (c). Solvent: CF_3COOD/D_2O.

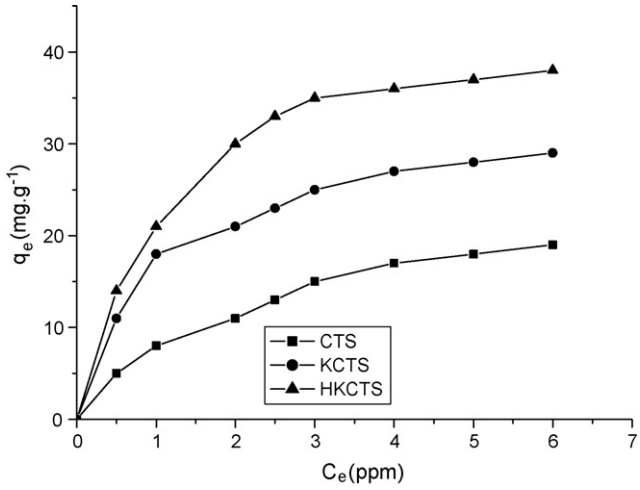

Fig. 4. The relationship of C_e and adsorption capacities.

3.3. Adsorption isotherms

The equilibrium adsorption of Zn(II) on chitosan derivatives as a function of the initial concentration of Zn(II) is shown in Fig. 4. It is seen that the adsorption capacity increase with increasing initial Zn(II) ion concentrations until equilibrium is attained. It also shows the adsorbing capacities for Zn(II) on KCTS and HKCTS are significantly higher than those on CTS. Adsorption isotherm is important to describe how solutes interact with adsorbent. The Langmuir and Freundlich models are often used to describe equilibrium sorption isotherms.

The most widely used Langmuir equation, which is valid for monolayer sorption onto a surface with a finite number of identical sites and is given by:

$$\frac{C}{q} = \frac{C}{q_0} + \frac{1}{q_0 b} \tag{2}$$

where q is the amount of Zn(II) adsorbed per unit weight of the chitosan derivatives at equilibrium concentration (mg g^{-1}), C the final concentration in the solution (mg l^{-1}), q_0 the maximum adsorption at monolayer coverage (mg g^{-1}), and b is the Langmuir constant related to the affinity of binding sites (ml mg^{-1}) and is a measure of the energy of adsorption. The experimental data are plotted as C/q versus C and are shown in Fig. 5. The Langmuir equation is found to satisfactorily describe the adsorption isotherms.

Alternatively, the experimental isotherm data are also modeled with the log-linearized Freundlich equation in the format (3):

$$\log q = \log k + \frac{1}{n}\log C \tag{3}$$

where q and C have the same definitions as in Eq. (2), k is a Freundlich constant representing the adsorption capacity, and n is a constant depicting the adsorption intensity (dimensionless). The plot of $\log q$ versus $\log C$ based on Eq. (3) for the same experimental results in Fig. 4 is shown in Fig. 6. Similarly to the Langmuir model, the Freundlich model can also fit the experimental adsorption isotherm data very well.

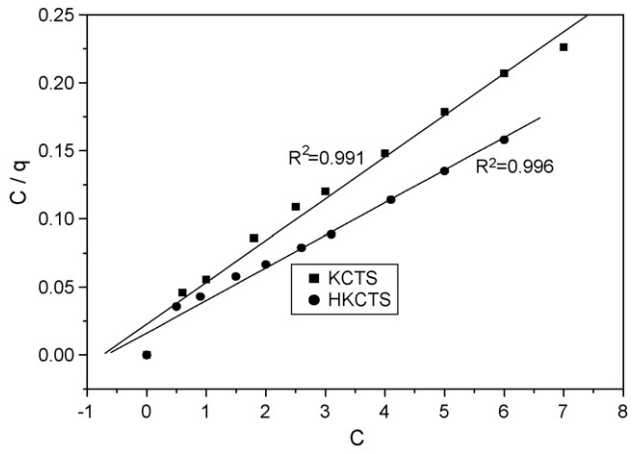

Fig. 5. Langmuir adsorption isotherm.

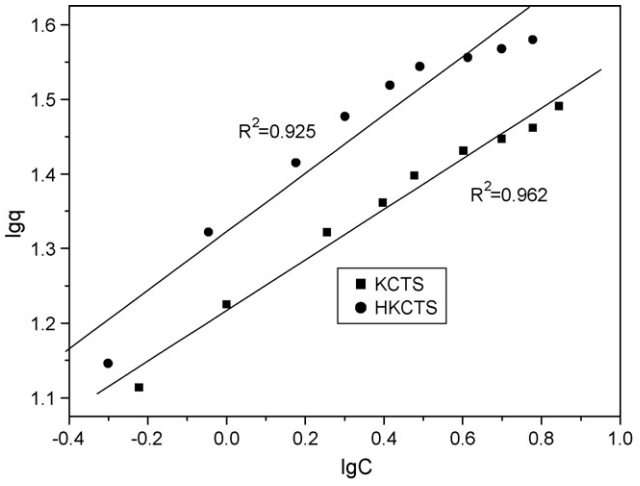

Fig. 6. Freundlich adsorption isotherm.

3.4. Kinetics of adsorption

Fig. 7 shows the time profiles of Zn(II) adsorption onto chitosan and chitosan derivatives. In the initial stage, the adsorption of Zn(II) significantly increased with increasing time. Hence, changes of the amounts of Zn(II) adsorbed decreased with the increasing time, and attained equilibrium at about 50 min for HKCTS and 60 min for KCTS. Because the mechanism of ion adsorption on porous adsorbents may involve three steps [12]: (i) diffusion of the ions to the external surface of adsorbent; (ii) diffusion of ions into the pores of adsorbent and (iii) adsorption of the ions on the internal surface of adsorbent. The first step of adsorption may be affected by metal ion concentration and agitation period. The last step is relatively a rapid process. The adsorption of Zn(II) remained constant after 50 min for KCTS and 60 min for HKCTS, implying that equilibrium had been reached. It is evident form Fig. 6 that the amount of adsorbate attained with CTS is smaller than the amount attained with chitosan derivatives are used.

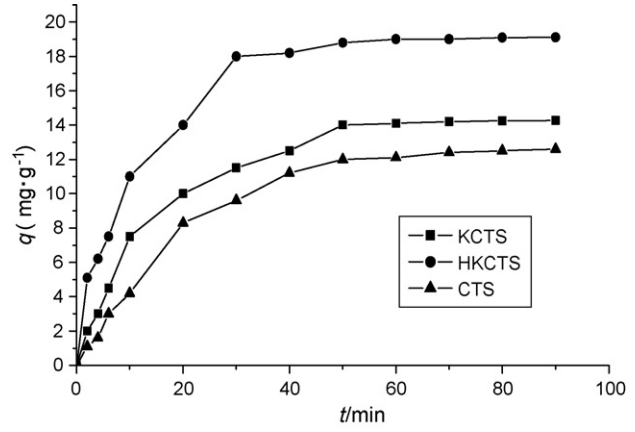

Fig. 7. The effect of reaction time on the adsorption of Zn^{2+}.

In order to investigate the controlling mechanisms of adsorption processes such as mass transfer and chemical reaction, the pseudo-first-order, second-order and intraparticle diffusion equations were used to test the experimental data [13–15]. The pseudo-first-order kinetic model are given as:

$$\log(q_e - q_t) = \log q_e - \frac{k_1}{2.303}t \tag{4}$$

where q_e and q_t are the amounts of Zn(II) adsorbed on adsorbent (mg g^{-1}) at equilibrium and at time t, respectively and k_1 is the rate constant of first-order adsorption (min^{-1}). Straight line plots of $\log(q_e - q_t)$ against t were used to determine the rate constant, k_1 and correlation coefficient R^2 values for Zn(II) under different concentration range conditions.

The pseudo-second-order equation may be expressed as:

$$\frac{t}{q_t} = \frac{1}{k_2 q_e^2} + \frac{t}{q_e} \tag{5}$$

where k_2 is the rate constant of second-order adsorption (g mg^{-1} min^{-1}). Straight-line plots of t/q_t against t were tested to obtain rate parameters and the results suggested the applicability of this kinetic model to fit the experimental data.

The intraparticle diffusion rate can be described as:

$$q_t = k_i t^{0.5} \tag{6}$$

where k_i is intraparticle diffusion rate (mg g^{-1} $min^{-0.5}$). The k_i is the slope of straight-line portions of the plot of q_t against $t^{0.5}$.

The results of the kinetic parameters for Zn(II) adsorption are shown in Figs. 8–10. Based on the correlation coefficients, the adsorptions of Zn(II) are best described by the pseudo-second-order equation. Many studies reported the first-order equation of Lagergren does not fit well to the initial stages of the adsorption processes. The first-order kinetic process has been used for reversible reaction with an equilibrium being established between liquid and solid phases [16]. Whereas, the pseudo-second-order kinetic model assumes that the rate-limiting step may be chemical adsorption [17]. In many cases, the

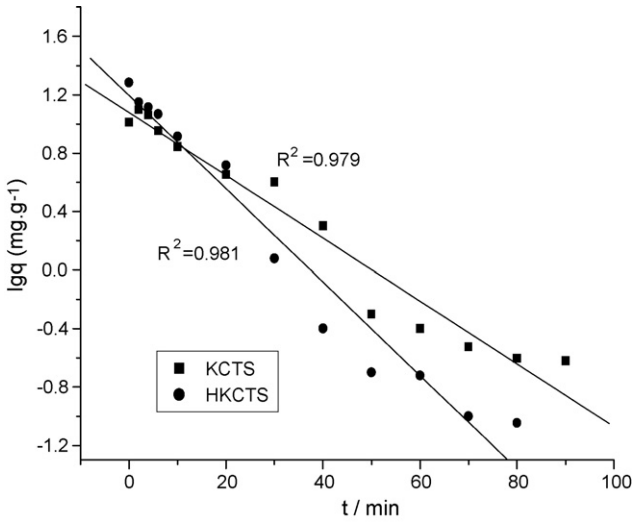

Fig. 8. Plot of the pseudo-first-order equation.

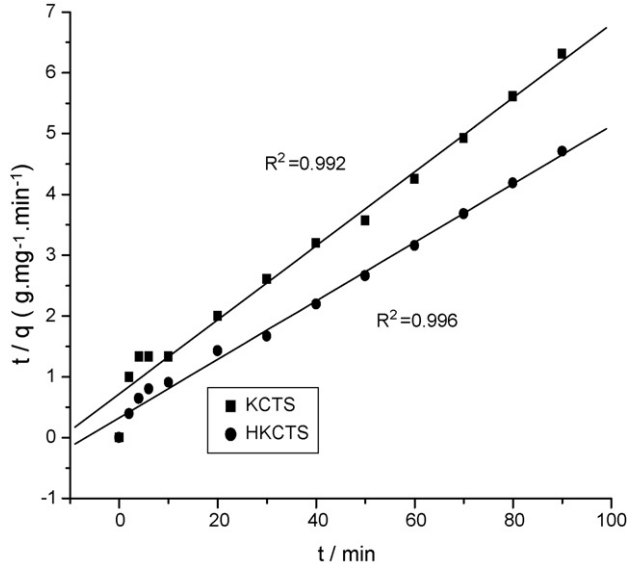

Fig. 9. Plot of the pseudo-second-order equation.

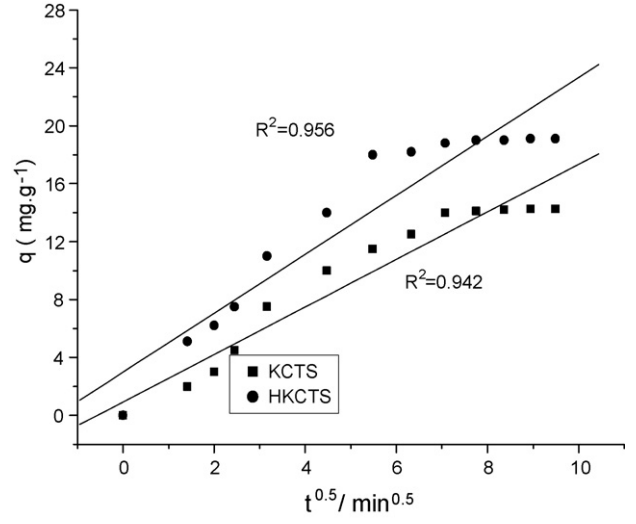

Fig. 10. Plot of the intraparticle diffusion equation.

pseudo-second-order equation correlates well to the adsorption studies.

3.5. Mechanism of chelating reaction chitosan derivatives with Zn(II) Ion

3.5.1. FT-IR analysis

Fig. 11 shows the FT-IR spectra of KCTS-Zn. The wide peak at 3442 cm^{-1} corresponding to the stretching vibration of $–NH_2$ group and –OH group shifted to lower frequency in the complexes, indicating $–NH_2$ or –OH groups take part in complexation. Absorption bands at 1580 cm^{-1} assigned to "free" amine group disappeared in the complexes. Instead, a new absorption band at 1384 cm^{-1} appeared, that was considered as characteristic peak of the association of KCTS and metal. It suggested that the amine or the acetamide group at C_2 interacted with metal. The peak at 1384 cm^{-1} attribute to bending vibration of –OH gradually disappeared in the KCTS-Zn complexes, indicating –OH take part in chelation.

The FT-IR spectrum of HKCTS-Zn polymeric matrix shows both carboxyl and amide carbonyls were shifted to lower frequencies upon complexation to zinc, i.e., from 1665 to 1560 cm^{-1} for amide carbonyls and from 1733 to 1680 cm^{-1} for carboxylic carbonyls, and the newly formed hydroxamic carbonyl groups at 1636 cm^{-1} in HKCTS-Zn were also shifted to lower frequencies upon complexation to zinc. Such shifts indicate that hydroxyl group in hydroxylamine, carboxyl group and amide group are coordinated to zinc ion. The band at 1110 and 660 cm^{-1} assigned to ionic SO_4^{2-} was found in all complexes' spectra, which indicated that SO_4^{2-} existed in the complexes in the ionic form.

3.5.2. XPS analysis

The XPS method was used to study the charge state of the metal in the course of catalytic transformations. The XPS binding energies obtained from the C 1s, O 1s, N 1s, Zn^{2+} $2p_{3/2}$ core levels of the diazine complexes are listed in Table 1.

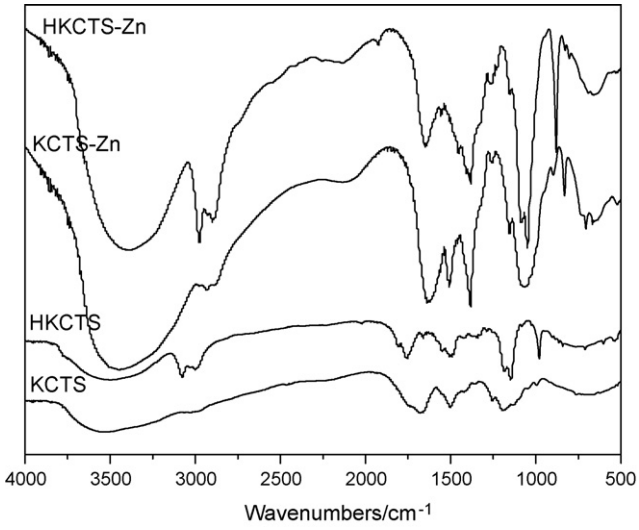

Fig. 11. FT-IR spectra for KCTS, KCTS-Zn, HKCTS and HKCTS-Zn.

Table 1
The binding energy of C 1s, O 1s, N 1s and Zn^{2+} $2p_{3/2}$ in samples

Sample	C 1s	O 1s	N 1s	Zn^{2+} $2p_{3/2}$
KCTS	284.60	531.6	398.8	
KCTS-Zn	284.61	531.6, 532.8	398.8, 399.1	1021.9, 1020.1
HKCTS	284.60	531.7	398.7	
HKCTS-Zn	284.62	531.7, 532.3, 532.6	398.7, 400.4	1021.9, 1020.6

The C 1s XPS spectra however did not clearly show significant changes of the C 1s BEs before and after Zn adsorption (less than 0.5 eV and the results not shown) (see Table 1). Since both FT-IR and XPS spectra could not provide clear evidence that the chemical bonds associated with the carbon atoms on both beads were significantly changed after Zn adsorption, it may be speculated that the contribution of Zn-carbon interaction to Zn adsorption on the beads was mainly through a non-specific interaction (physical adsorption, electrostatic attraction, etc.) or a very weak chemical interaction. Therefore, C atom does not take part in complexation.

Figs. 12c and 13c show the typical XPS wide scan spectra for chitosan derivatives before and after Zn adsorption. It is clear that a new peak at the BE of about 1020.1 ev for KCTS or 1020.6 ev for HKCTS appeared after Zn adsorption. The presence of a satellite band nearly is representative of the oxidation state +2 for the Zn $2p_{3/2}$ orbital. Therefore, the peak at BE of 1020.1 ev for KCTS or 1020.6 ev for HKCTS provides evidence of Zn^{2+} being adsorbed on the surface of KCTS and HKCTS.

In Figs. 12b and 13b, the typical N 1s XPS spectra of KCTS and HKCTS before and after Zn adsorption are presented. Before Zn adsorption, there is only one peak at 398.8 eV for KCTS or at 398.7 eV for HKCTS. This is attributed to the N atom in the $–NH_2$ and/or the –NH– groups on the surfaces of KCTS and HKCTS. After Zn adsorption, however, a new peak at BE of 399.1 eV for KCTS or at BE of 400.4 eV for HKCTS is observed. This indicates that some N atoms existed in a more oxidized state on the beads' surfaces due to Zn adsorption. This phenomenon can be attributed to the formation of $R–NH_2Zn^{2+}$ complexes, in which a lone pair of electrons in the nitrogen atom was donated to the shared bond between the N and Zn^{2+}, and, as a consequence, the electron cloud density of the nitrogen atom was reduced, resulting in a higher BE peak observed. Therefore, the XPS spectra provide evidence of Zn binding to nitrogen atoms, in agreement with the FT-IR findings.

The O 1s spectrum of KCTS could be decomposed into two single peaks (see Fig. 12a) with assignments of 531.6 eV as carboxyl oxygen atoms (–CO–O–), 532.8 eV as methylene bound to one oxygen atom ($–CH_2–O–$). The O 1s spectrum of HKCTS had three components (see Fig. 13a) at 531.7, 532.3, and 532.6 eV, attributed to $–CH_2–O–$, –CO–O–, and –NH–O– oxygen, respectively. This indicates that the oxygen in carboxyl group of KCTS were coordination atoms. Oxygen atom of hydroxamic acid and oxygen atom of carbonyl group in HKCTS coordinated with Zn^{2+}, in agreement with the FT-IR findings.

Based on the analysis above, we speculate the molecular structure of chitosan derivatives-metal complexes as follow (Fig. 14).

Through the discussion upon the mechanisms and kinetics of chitosan derivatives-metal complexes, it is concluded that chitosan derivatives shows effective sorption to metal ions. Therefore, chitosan derivatives can be used as effective absorbent for metal ions removal from water and industrial effluents. Chitosan derivatives are inexpensive and easily available in large quantity, and their use as absorbent would significantly lower the cost of wastewater treatment.

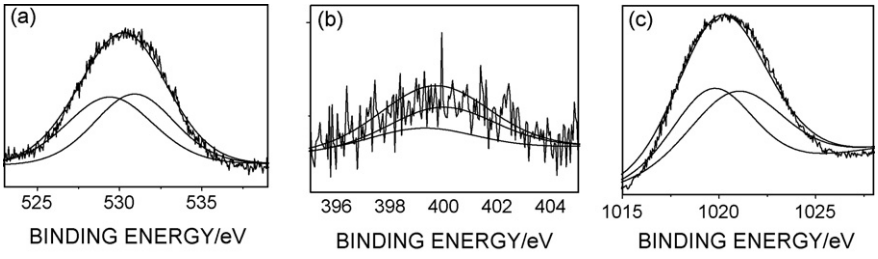

Fig. 12. The XPS spectra of O 1s (a), N 1s (b) and Zn^{2+} $2p^3$ (c) of KCTS-Zn.

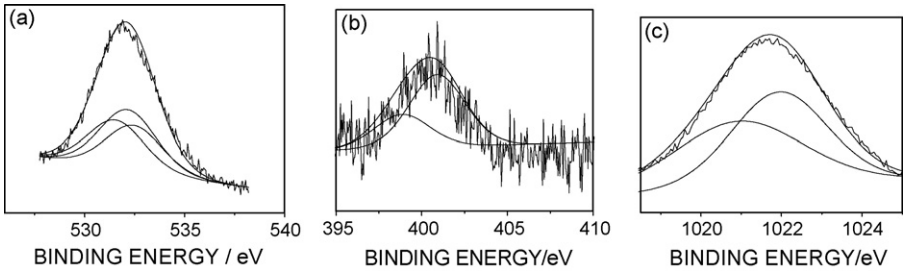

Fig. 13. The XPS spectra of O 1s (a), N 1s (b) and Zn^{2+} $2p^3$ (c) of HKCTS-Zn.

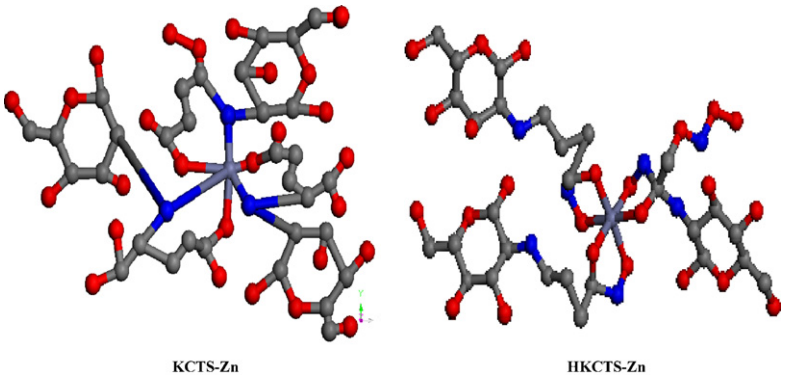

Fig. 14. Possible Structure of KCTS-Zn and HKCTS-Zn: (N), (C), (O), (Zn).

4. Conclusions

In this study, the capacity of chitosan derivatives to adsorb Zn(II) ions from aqueous solutions was examined, including equilibrium and kinetic studies. The adsorption process could be best described by the second-order equation. This suggests that the rate-limiting step may be the chemical adsorption not the mass transport. The mechanisms of chelating reaction between chitosan derivatives and Zn(II) are investigated by infrared spectral analysis and X-ray photoelectron spectroscopy analysis. The novel chitosan derivatives have high adsorption capacity, it is predicted that these chitosan derivatives will have wide-ranging applications in the sequestration or removal of metal ions and many other industrial processes.

Acknowledgment

This work was supported by research grants from the National Science Foundation of China (Project No. 20376085).

References

[1] G.A.F. Roberts, Chitin Chemistry, Macmillan Press, London, 1992.
[2] C.J. Brine, P.A. Sandford, J.P. Zikakis, Advanced Chitin and Chitosan, Elsevier, New York, 1992.
[3] E. Guibal, C. Milot, J.M. Tobin, Metal-anion sorption by chitosan beads: equilibrium and kinetic studies, Ind. Eng. Chem. Res. 37 (1998) 1454–1463.
[4] W.S.W. Ngah, S.A. Ghani, L.L. Hoon, Comparative adsorption of lead(II) on flake and bead-types of chitosan, J. Chin. Chem. Soc. 49 (2002) 625–628.
[5] M.S. Chiou, H.Y. Li, Equilibrium and kinetic modelling of adsorption of reactive dye on crosslinked chitosan beads, J. Hazard. Mater. B 93 (2002) 233–248.
[6] X.F. Zeng, E. Ruckenstein, Cross-linked macroporous chitosan anion-exchange membranes for protein separations, J. Membr. Sci. 148 (1998) 195–205.
[7] M. Terbojevich, A. Cosani, R.A.A. Muzzarelli, Molecular parameters of chitosans depolymerized with the aid of papain, Carbohydr. Polym. 29 (1996) 63–68.
[8] E. Guibal, Interactions of metal ions with chitosan-based sorbents: a review, Sep. Purif. Tech. 38 (2004) 43–74.
[9] A.J. Varmaa, S.V. Deshpandea, J.F. Kennedy, Metal complexation by chitosan and its derivatives: a review, Carbohydr. Polym. 55 (2004) 77–93.
[10] B. Krajewska, Application of chitin- and chitosan-based materials for enzyme immobilizations: a review, Enzyme Microb. Tech. 35 (2004) 126–139.
[11] Z. Zong, Y. Kimura, M. Takahashi, H. Yamane, Characterization of chemical and solid state structures of acylated chitosans, Polymer 41 (2000) 899–906.
[12] C. Peniche-Covas, L.W. Alvarez, W Arguelles-Monal, The adsorption of mercuric ions by chitosan, J. Appl. Polym. Sci. 46 (1992) 1147–1150.
[13] W.S.W. Ngah, S.A. Ghani, A. Kamari, Adsorption behaviour of Fe(II) and Fe(III) ions in aqueous solution on chitosan and cross-linked chitosan beads, Bioresour. Technol. 96 (2005) 443–450.
[14] Y.S. Ho, G. McKay, Sorption of dye from aqueous solution by peat, J. Chem. Eng. 70 (2) (1998) 115–124.
[15] Y.S. Ho, G. McKay, The kinetics of sorption of divalent metal ions onto sphagnum moss peat, Water Res. 34 (2000) 735–742.
[16] K.S. Low, C.K. Lee, S.C. Liew, Sorption of cadmium and lead from aqueous solutions by spent grain, Process Biochem. 36 (2000) 59–64.
[17] F.C. Wu, R.L. Tseng, R.S. Juang, Enhanced abilities of highly swollen chitosan beads for color removal and tyrosinase immobilization, J. Hazard. Mater. B 81 (2001) 166–177.